Available online at www.sciencedirect.com
ScienceDirect
Biochemical and Biophysical Research Communications 351 (2006) 7–13
BBRC
www.elsevier.com/locate/ybbrc

Reduction in nonfluorescence state of quantum dots on an immunofluorescence staining

Songhua Li-Shishido [a], Tomonobu M. Watanabe [b], Hiroshi Tada [a], Hideo Higuchi [b,*], Noriaki Ohuchi [a]

[a] *Division of Surgical Oncology, Graduate School of Medicine, Tohoku University, Japan*
[b] *Biomedical Engineering Research Organization, Tohoku University, Japan*

Received 8 September 2006
Available online 9 October 2006

Abstract

Fluorescence quantum dots are widely used in immunofluorescence staining because of their intense and stable fluorescence. However, the nonfluorescence state of the quantum dots is their disadvantage. Here, the nonfluorescence state of the dots labeled to cells and tissues was suppressed. Cells and tissues where the receptor HER2 had been overexpressed were fixed and then labeled with anti-HER2 cross-linked with the dots. The intensity of the dots increased with the illumination time. The majority of the single dots were in the nonfluorescence state at beginning of the illumination period and the number of fluorescence dots observed increased with the illumination time. Living cells were also labeled with the anti-HER2-Qdots. Blinking and bleaching of the Qdots was effectively suppressed by adding β-mercaptoethanol and glutathione. Therefore, the movement of the Qdots bound to cell membrane could be observed for long periods of time.

Keywords: Quantum dots; Immunofluorescence; Fixed cell; Fixed tissue; Live cell; Imaging; Single particles; Single molecules; Nanotechnology

The fluorescence quantum dots (Qdots) are nanocrystals of semiconductor materials, for example, CdSe and CdTe [1–4]. The wavelength of the fluorescence of the Qdots changes with the diameter of the crystals. Small sized crystals (~2 nm in diameter of CdSe) emit blue fluorescence and larger crystals (~4 nm) emit red fluorescence [1]. The quantum yield of fluorescence emission is affected by the environmental conditions [5]. To get higher quantum yield of fluorescence, the Qdots were coated with the other semiconductor, for example, ZnS [5]. For use in biological experiments, the Qdots were coated further with a polymer which has reactive sites, amine or carboxyl groups, to conjugate with proteins, DNA and RNA [6]. After conjugation, the Qdots are imaged to determine the localization of target biological molecules and measure the number of target molecules [7–9].

The fluorescence intensity of the Qdots is considerably higher than that of organic dyes. They do not bleach for long period of time even in the absence of anti-fading reagents, which would destroy cell [8]. These advantages of the Qdots have been widely used in the biological and medical fields [3,10]. The disadvantage of the Qdots is that they bind reversibly to a nonfluorescence state which results in blinking and low fluorescence intensity [11–13]. To measure the number or intensity of the Qdots that have bound to cells, the intensity of each Qdot must be stable. To observe single Qdots labeled to proteins for long periods of time, the Qdots must emit fluorescence for long periods without blinking [13,14].

In this study, the nonfluorescence state (off-state) of the antibody–Qdot complex bound to the cells was reduced in order to improve the quantitative measurements and fluorescence period of the Qdots. The period at fluorescence

* Corresponding author. Fax: +81 22 795 5753.
E-mail address: higuchi@tubero.tohoku.ac.jp (H. Higuchi).

0006-291X/$ - see front matter © 2006 Elsevier Inc. All rights reserved.
doi:10.1016/j.bbrc.2006.09.159

state (on-state) of the Qdots bound to fixed and embedded cells increased with the time when that were illuminated by laser. The reducing agents, β-mercaptoethanol or glutathione, were inhibited the off-state.

Materials and methods

Qdot was conjugated to chimeric monoclonal antibody against HER2, trastuzumab (Herceptin, Chugai Pharmaceutical Ltd.) with Qdots 605, 655, and 705, where the number indicates the wavelength at maximum fluorescence. An antibody Conjugation Kit (Qdot corporation) was used [7,15] according to the manufacturer's instructions. The final concentration of trastuzumab–Qdots was determined by measuring the conjugate absorbance.

The human breast cancer cell line KPL-4, which overexpresses HER2 and is sensitive to trastuzumab [16,17], was kindly provided by Dr. J. Kurebayashi. KPL-4 cells were cultured in DMEM supplemented with 5% fetal bovine serum. MDA-MB-231 cells having a low expression of HER2 were maintained in L-15 medium, respectively, with 10% fetal bovine serum [16,18,19].

A suspension of KPL-4 cells was transplanted subcutaneously to the dorsal skin of female Balb/c nu/nu mice at ~5 weeks of age (Charles River). Several weeks after tumor inoculation, mice bearing a tumor with a volume of 100–200 mm^3 were selected. The mice were sacrificed with an overdose of CO_2. The tumors were removed and divided. All operations on animals were in accordance with the institutional animal use and care regulations.

For the immuno histochemical analysis, cells on a coverslip were fixed at 10% neutral-buffered formalin for 10 min [8]. Fixed cells were extensively washed three times with PBS solution. To minimize the nonspecific binding of trastuzumab-Q dot complexes to the cells, the cells were treated with the blocking solution containing NH_4Cl, glycine, FBS or BSA. The best treatment for blocking was incubating the cells in PBS solution containing 50 mM NH_4Cl for 10 min and then in 10% FBS for 30 min after a through washing with NH_4Cl.

The trastuzumab–Qdot complexes or polyclonal anti-HER2 cells from rabbit were reacted with the cells that had been blocked. The anti-HER2 cells were further reacted with anti-rabbit IgG conjugated with Qdots.

Tumors were fixed in 10% neutral-buffered formalin overnight [8] and then transferred into ethanol before processing and paraffin embedding. The tissue after removing paraffin was then treated with the PBS solution containing trastuzumab–Qdots. The fixed cells and tissue were embedded into Permafluor™ (Thermo Shandon).

Qdots were observed under microscopes (IX71 or BX51, Olympus) [20,21], equipped with green laser (532 nm), long pass filter (>580 nm). Fixed cells were observed at a power density of 11 (Fig. 1), or 31 W/mm^2 (Figs. 2–4). The x- and y-positions of the fluorescent spot were calculated by fitting the data to a 2D-Gaussian curve [21].

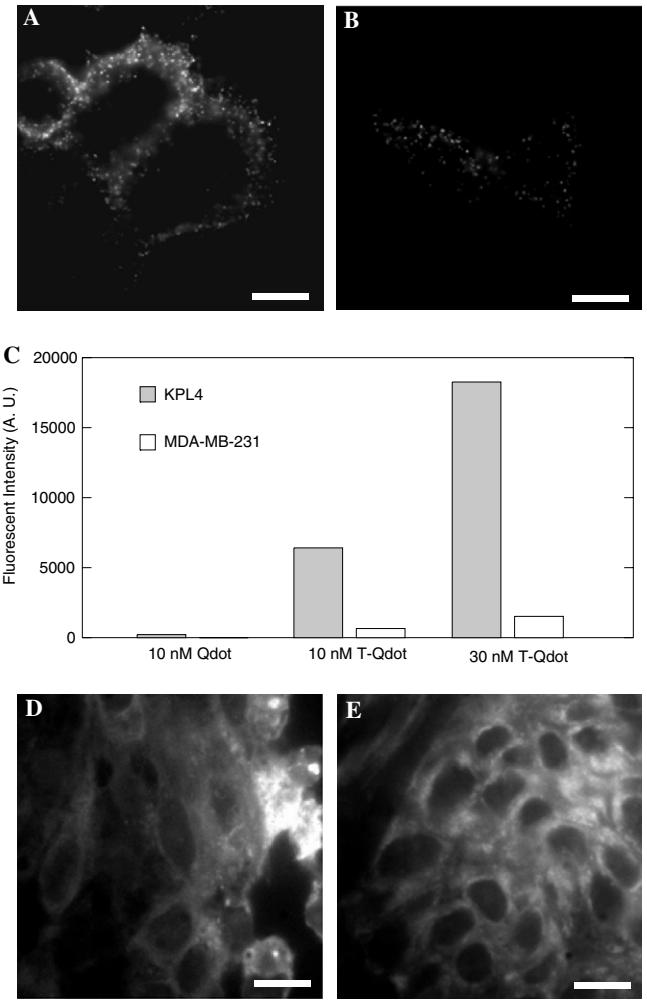

Fig. 1. Antibody–Quantum dot complex bound to cells and the tumor. Qdot705 (30 nM) labeled with trastuzumab bound to fixed KPL-4 cells (A) and MDA-MB-231 cells (B). (C) Fluorescence intensity of Qdots measured in several different cells. Open and closed bars indicate the intensity of KPL-4 and MDA-MB-231 cells, respectively. The two bars on the left-hand side show Qdots that have not bound trastuzumab after they had been mixed with the cells. Bars in the center and on the right show results in the presence of trastuzumab. (D) Sections of a tumor in a mouse, 5 μm thickness, were stained using Qdot-705 (10 nM) and labeled with trastuzumab. (E) The section was reacted with rabbit anti-HER2 and then with Qdot-705 (10 nM) labeled with anti-rabbit IgG. Scale bars = 10 μm (A, B, D, and E). Images were taken at an exposure time of 0.2 s at laser power of 11 W/mm^2.

Results

The trastuzumab–Qdots bound well to KPL-4 cells but not to the MDA-MB-231 cells which expressed HER2 at low levels [19] (Fig. 1A and B). Most of the Qdots bound to the cell membrane (Fig. 1A). The intensity of the Qdots bound to the cells was measured in order to estimate the number of the bound Qdots. The Qdots without trastuzumab labeling did not bind to KPL-4 and MDA-MB-231 cells (Fig. 1C). The intensity of the Qdots bound to KPL-4 was approximately 10 times higher than those bound to MDA-MB-231 cells. This result was consistent with the expression of HER2 in these cells [19].

The trastuzumab–Qdots were bound to a tumor transplanted in a nude mouse. The trastuzumab–Qdots bound mainly to the region near the KPL-4 cell membrane (Fig. 1D). The tumor also reacted with the polyclonal anti-HER2 cells from rabbits and then with anti-rabbit IgG labeled with the Qdots (Fig. 1E). The rabbit-IgG–Qdots bound to the cell membrane in similar areas where the trastuzumab–Qdots bound using direct staining methods (Fig. 1D and E). These results indicate that the fixed cells and tumor cells could be successively stained with antibodies labeled with the Qdots.

The change in fluorescence intensity of the antibody–Qdots was measured after illuminating the sections for long periods by a laser to test the stability of fluorescence emis-

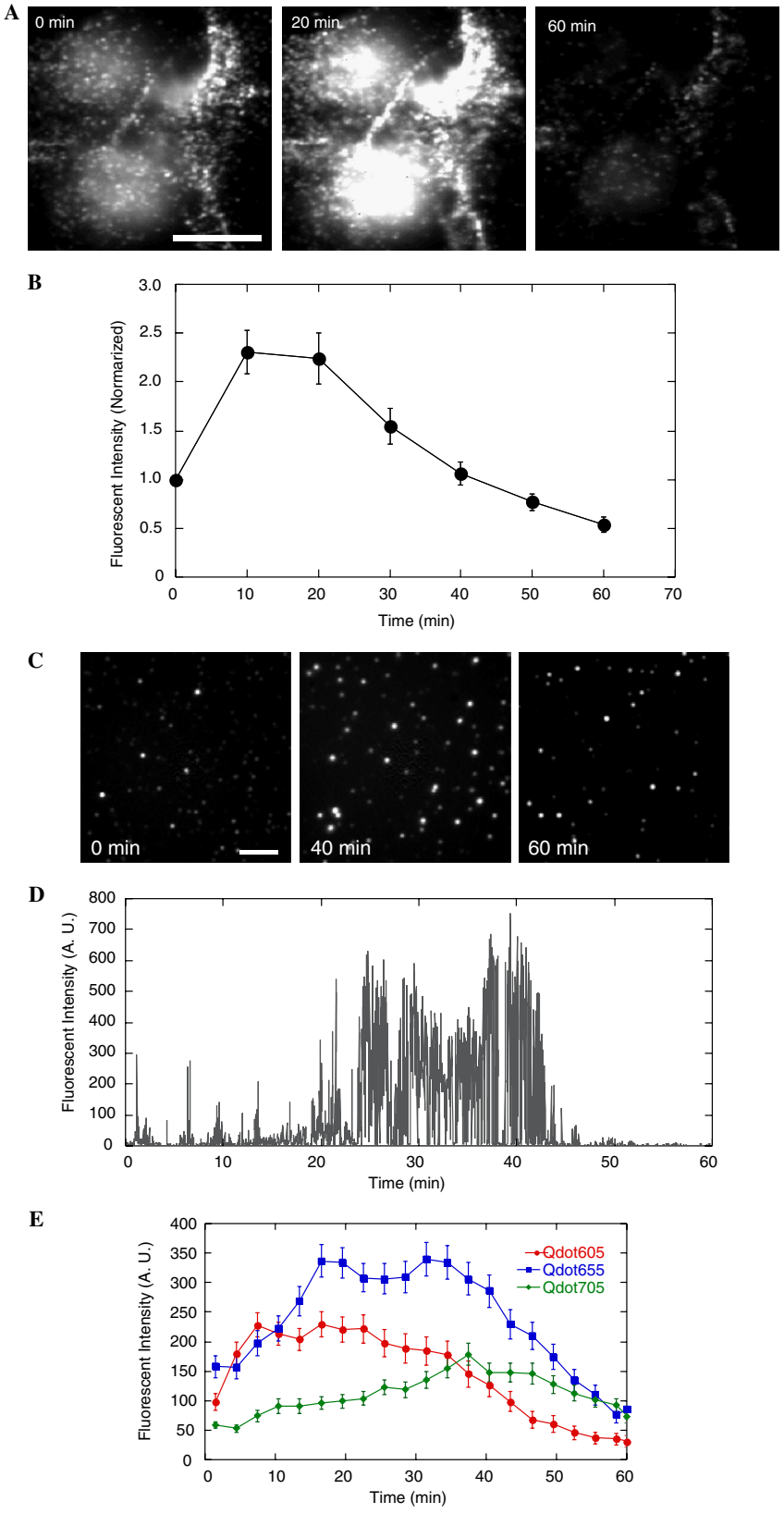

Fig. 2. Change in Qdot intensity when illuminated by a green laser. KPL-4 cells were labeled with trastuzumab–Qdot-705 (10 nM). Qdots were illuminated by the green laser at a laser power of 74 W/mm^2. (A) Images were taken at an exposure time of 0.05 s at illumination periods of 0, 20, and 60 min. Scale bar indicates 10 μm. (B) Intensity in several regions were measured. (C) Trastuzumab–Qdots-705 (0.1 nM) were spread on a coverslip. Images were taken at exposures time of 1 s at illumination periods of 0, 40, and 60 min using a laser power of 74 W/mm^2. Scale bar = 10 μm. (D) Intensity at several regions was measured at an exposure time of 1 s. (E) The average of hundreds of intensities from Qdots-605 (red symbols), 655 (blue), and 705 (green).

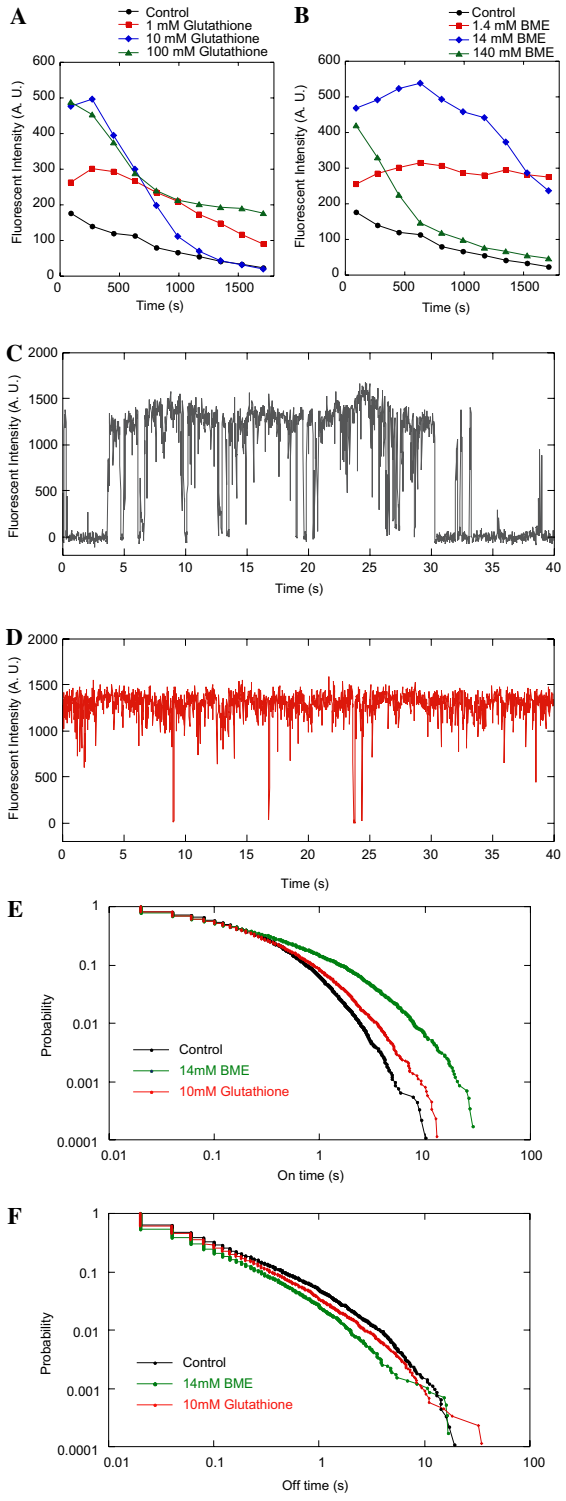

Fig. 3. The on- and off-dwell times in the presence of reducing agents. Qdot-655 (0.1 nM) in PBS solution containing BME (0, 1.4, 14, and 140 mM, (A)) and glutathione (0, 1, 10, and 100 mM, (B)) were spread on coverslips. Images were taken at exposure time of 1 s for 30 min at a laser power of 74 W/mm^2. (C,D) Images in the absence (C) and presence (D) of 14 mM BME were taken at beginning of the illumination period at exposure times of 20 ms and a laser power of 74 W/mm^2. (E,F) Fluorescence of the on- and off- dwell times was measured from the results shown in (C) and (D). The total dwell time was calculated from the probability.

sion. The power of green laser was increased by ~ 7 times to accelerate the intensity change. The intensity increased prominently 20 min into the illumination period (Fig. 2A). Sixty minutes into the illumination period, the intensity had returned to its original levels. The intensities at many regions in cells could be quantitatively analyzed relative to the initial intensity (Fig. 2B). In contrast, the fluorescence intensity of an organic fluorescence molecule, Cy3, conjugated to trastuzumab decreased exponentially with the illumination time (data not shown). The time constant was only 20 s.

To find the reason for this enhancement of intensity, the intensity of single Qdots embedded into Permafluor™ without being attached to cells was analyzed. Sequential images were taken every 1 s (Fig. 2C). The number of fluorescence Qdots appeared to increase, while the intensity of the bright Qdots changed little (Fig. 2C). Fig. 2D shows the intensity change in relation to the illumination time. The intensity of most Qdots increased firstly and decreased with time. During the periods where the Qdots exhibited their highest intensity, i.e., 20–43 min after the start of the illumination period (Fig. 2D), Qdots blinked from zero to maximum intensity. Assemble averages of the intensity of Qdot-705 showed that the intensity increased at the beginning and then gradually decreased to the end (Fig. 2E). The other Qdots, 605 and 705, showed similar intensity profiles to the Qdot-655 but had different time constants.

Fluorescence imaging is also used for position measurements of proteins [21,22]. To observe the position of Qdots bound to living cells, we determined the most suitable conditions that allowed Qdots to bind for long periods of time with high spatial and temporal precision [21]. The reducing reagent, DTT and β-mercaptoethanol (BME), are known to suppress the blinking but its effects on the bleaching time have not been determined [13]. We investigated the effect of BME and glutathione on both the bleaching and blinking. The intensity increased several fold in the presence of the reducing agents comparing to that in the absence (Fig. 3A and B). The intensity decreased with the time illuminated by the laser. The intensity in the presence of 1 and 100 mM glutathione, 1.4 and 14 mM BME suppressed the reduction of intensity for long time (30 min). In the presence of 10 mM glutathione and 140 mM BME, the intensity was reduced only at the beginning (<20 min) and not thereafter.

To analyze the blinking of the fluorescence intensity, the temporal resolution of the imaging was improved to be 20 ms (Fig. 3C and D). In the absence of the reducing agent, the Qdots blinked frequently and showed long dwell times in the off-state. In the presence of BME, the Qdots emitted the fluorescence continuously for long periods of time without spending long periods in the off-state. To evaluate the suppression of blinking, the dwell times of on and off-states were analyzed [13]. The probability of Qdots being in the state of long on-dwell time in the presence of BME is much higher than that in the absence of BME. For example, the probabilities of Qdots having on-

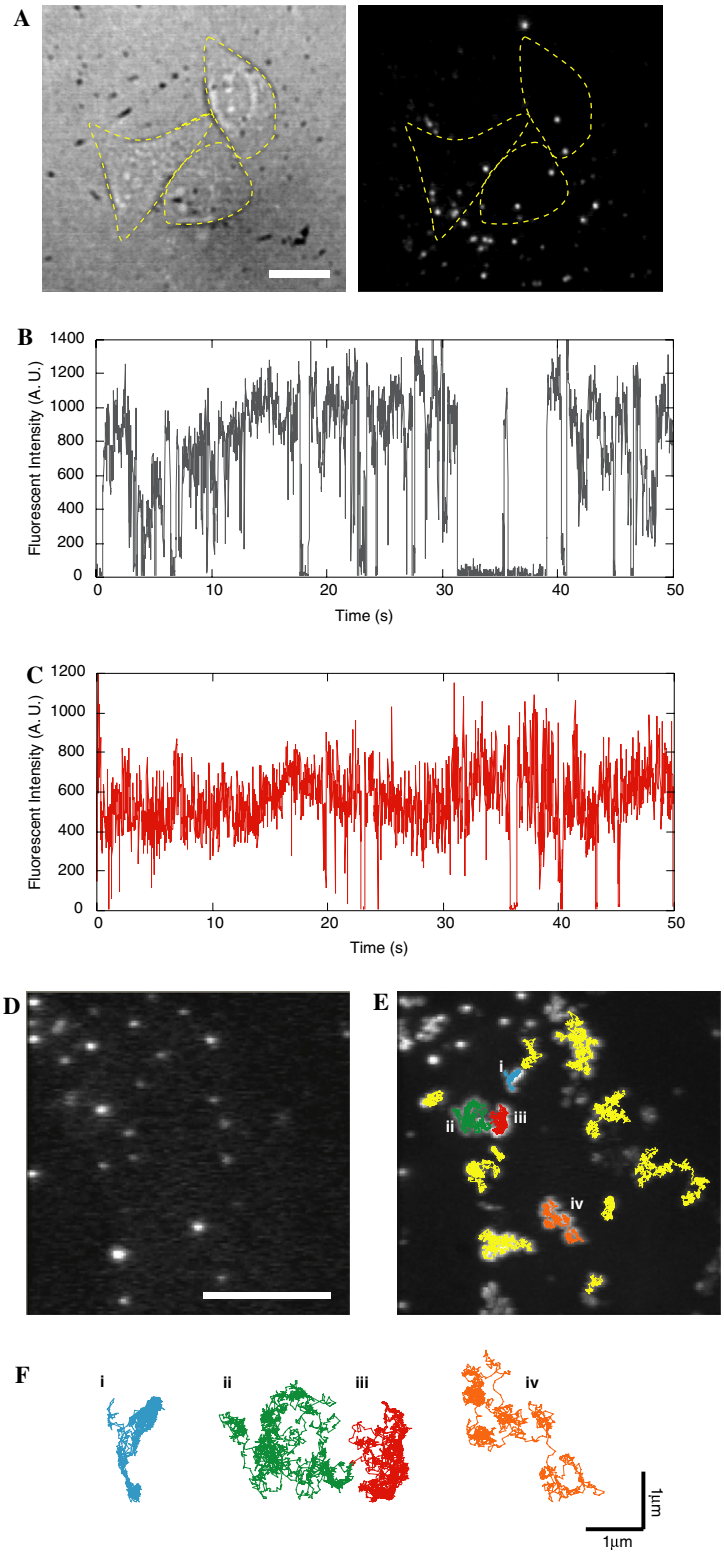

Fig. 4. Blinking of Qdots bound to living cells. Qdots-655 (0.5 nM) labeled with trastuzumab were bound to living KPL-4 cells. (A) There are a bright field (left) and fluorescence (right) images of the cells. Dotted lines indicate the edge of the cells. Scale bar = 10 μm. The blinking of Qdots in the absence (B) and presence (C) of 14 mM BME is shown at an exposure time of 20 ms. (D) Fluorescence images of Qdots were taken under a total internal reflection microscope at an exposure time of 20 ms and laser power of ~70 W/mm^2. Scale bar = 5 μm. (E) The Qdots bound to cells were taken at a higher magnification. To trace the movement of Qdtos, 2500 images were collected over a 50 s period and then superimposed. Colored lines indicate the traces of single Qdots. (F) Traces indicate movements of Qdots that occurred on the cell membrane for a 50 s period.

dwell times of 5 s are approximately 2.3% in the presence of BME which are considerably higher than 0.10% in the absence of BME. The off-dwell time is also higher in the absence of BME. Long on-dwell times and short off-dwell times observed in the presence of BME indicate that the Qdots stay in the on-state for most of the time.

The imaging of proteins in living cells is an important application of Qdots. The trastuzumab–Qdot complexes were mixed with living cells to detect the movement of membrane receptor, HER2, in the presence of BME. The movement of the Qdots was measured within the first 30 min when the activity of the cells was not altered.

The trastuzumab–Qdot complexes bound to the membrane of the cells (Fig. 4A). Qdots in the absence of BME often exhibited blinking (Fig. 4B). Most on-dwell times were less than 1 s. The long off-dwell times were common. In the presence of 14 mM BME, the on-dwell times became longer than 1 s for many of the Qdots (Fig. 4C). The off-dwell time was very short <0.2 s (Fig. 4C).

The position of the Qdots bound to cell membrane was measured by fitting the data of the fluorescence of the spots to two-dimensional Gaussian with one nanometer precision [21,23]. Fig. 4D shows the initial image of the Qdots bound to the cell membrane. All images have been superimposed as shown in Fig. 4E. The center of the fluorescence spots was measured continuously for 50 s without losing the data by off-dwell (colored traces in Fig. 4E). Traces on an expanded time scale show the detailed movement of the Qdots (Fig. 4F). Most of the Qdots moved a distance of 3 μm in 50 s which is considerably shorter than that of free diffusion of trastuzumab–Qdots ($\sim$30 μm assuming the diameter of 30 nm). The some of movements of the Qdots were random (Fig. 4F(i and ii)). Some of the Qdots moved within a narrow area (iii). Other Qdots moved within small area and then hoped to the next area (iv).

Discussion

The intensity of the Qdots bound to KPL-4 cells was approximately 10 times higher than that to MDA-MB-231 cells. This result is consistent with the expression HER2 in these cells [16,18,19]. The advantage of Qdot immunofluorescence staining is that quantitative analysis of bound Qdots to cells is possible. Another advantage is the higher sensitivity as even single Qdots can be imaged (Figs. 2C and 4D) [13,14,21]. The trastuzumab–Qdots also bound selectively to a tumor formed by KPL-4 cells transplanted in a nude mouse, suggesting this technique has applications for medical immunohistochemistry [3,24,25].

Organic fluorescent dyes for immunofluorescence staining are not suitable for quantitative analysis because of their low intensity and rapid bleaching within 20 s of illumination [8]. The trastuzumab–Qdots remained stable for periods up to 1 h (Fig. 2) [8,13,26,27]. The intensity of the Qdots did not change much in the first $\sim$10 min after laser illumination (Fig. 2E). The intensity then gradually increased to 2–3 times of from the initial intensity and then decreased [26]. These changes in intensity were also obtained for Qdots labeled cells stored in the Permafluor for 3 months at room temperature (data not shown). These results indicate that Qdots are very useful for quantitative analysis of immunofluorescence staining even when they have been stored for long periods.

Measurements of the intensity of single Qdots indicated that the number of Qdots at the fluorescence on-state increases with time (Fig. 2). The single Qdots were bleached by long-term continuous illumination with a laser. These changes in intensity of single Qdots explain the change in intensity of multiplied Qdots bound to cells (Fig. 2). Single Qdots analysis is a powerful method to determine the fundamental properties of Qdots [14,21].

The reducing agents, BME and DTT, suppressed the blinking of intensity of Qdots [13]. The intensity of Qdots in the presence of BME and glutathione was measured. BME (1.4 mM or higher) and glutathione (1 mM or higher) considerably enhanced the on-dwell time and shortened the off-dwell time marginally. The on-dwell time was enhanced in the presence of 14 mM BME but not in the presence of 140 mM BME. The enhancement of on-dwell time by the reducing agents was consistent with the previous results [13].

The longer on-dwell times and shorter off-dwell times increased the possibility that Qdots would stay in the on-state (Fig. 3C–F). Therefore, the total intensity of Qdots increased considerably at the beginning of the illumination period (Fig. 3A and B). Illumination for long periods using a laser resulted in the Qdots bleaching and the total intensity gradually decreasing. The decay time of the intensity by photobleaching was slowest in the presence of 14 mM BME. At higher concentrations of BME (140 and 280 mM), the intensity decay time was shorter. The optimum conditions for suppressing the bleaching and blinking were 14 mM BME.

Qdots bind to proteins in both *in vitro* motility assays and in cells [14,21]. The higher intensity of the fluorescence has made it possible to precisely detect the position of Qdot within a few nanometers and milliseconds. Because many of Qdots did not exhibit the blinking for >10 s, the Qdot position was measured for long time without missing the data by blinking (Fig. 4D–F). The movements of Qdots are much slower than that at free diffusion. Some of Qdots showed the hopping movement from the one area to the other, which is consistent with previous reports [28].

Stable and intense fluorescence of Qdots are advantageous for fluorescence imaging. However, blinking and non-specific binding of Qdots must be acknowledged as potential problems. Here non-specific binding was avoided by the improvement of blocking method. The off-state of Qdots bound to fixed and embedded cells was suppressed by the illumination of laser. The blinking of Qdots bound to living cells were suppressed effectively in the presence of 14 mM BME. These improvements open-up the new applications of Qdots such as medical immunostaining and nanometer measurement of position.

Acknowledgments

We thank Ms. Sachiko Higuchi and Dr. J.M. West for helping. This work was supported by Grants-in-Aid for Research Project, Promotion of Advanced Medical Technology (N.O.), Scientific Research in Priority Areas from the Japan MEXT (H.H.), and Special Coordination Funds for Promoting Science and Technology of Japan (H.H., T.M., and N.O.).

References

[1] M. Bruchez Jr., M. Moronne, P. Gin, S. Weiss, A.P. Alivisatos, Semiconductor nanocrystals as fluorescent biological labels, Science 281 (1998) 2013–2016.
[2] W.C. Chan, S. Nie, Quantum dot bioconjugates for ultrasensitive nonisotopic detection, Science 281 (1998) 2016–2018.
[3] X. Gao, Y. Cui, R.M. Levenson, L.W. Chung, S. Nie, In vivo cancer targeting and imaging with semiconductor quantum dots, Nat. Biotechnol. 22 (2004) 969–976.
[4] X. Michalet, F.F. Pinaud, L.A. Bentolila, J.M. Tsay, S. Doose, J.J. Li, G. Sundaresan, A.M. Wu, S.S. Gambhir, S. Weiss, Quantum dots for live cells, in vivo imaging, and diagnostics, Science 307 (2005) 538–544.
[5] X. Peng, M.C. Schlamp, A.V. Kadavanich, A.P. Alivisatos, Epitaxial growth of highly luminescent CdSe/CdS core/shell nanocrystals with photostability and electronic accessibility, J. Am. Chem. Soc. 119 (1997) 7019–7029.
[6] W.C. Chan, D.J. Maxwell, X. Gao, R.E. Bailey, M. Han, S. Nie, Luminescent quantum dots for multiplexed biological detection and imaging, Curr. Opin. Biotechnol. 13 (2002) 40–46.
[7] I.L. Medintz, H.T. Uyeda, E.R. Goldman, H. Mattoussi, Quantum dot bioconjugates for imaging, labeling and sensing, Nat. Mat. 4 (2005) 435–446.
[8] X. Wu, H. Liu, J. Liu, K.N. Haley, J.A. Treadway, J.P. Larson, N. Ge, F. Peale, M.P. Bruchez, Immunofluorescent labeling of cancer marker Her2 and other cellular targets with semiconductor quantum dots, Nat. Biotechnol. 21 (2003) 41–46.
[9] D.S. Lidke, P. Nagy, R. Heintzmann, D.J. Arndt-Jovin, J.N. Post, H.E. Grecco, E.A. Jares-Erijman, T.M. Jovin, Quantum dot ligands provide new insights into erbB/HER receptor-mediated signal transduction, Nat. Biotechnol. 22 (2004) 198–203.
[10] B.N. Giepmans, T.J. Deerinck, B.L. Smarr, Y.Z. Jones, M.H. Ellisman, Correlated light and electron microscopic imaging of multiple endogenous proteins using Quantum dots, Nat. Methods 2 (2005) 743–749.
[11] M. Nirmal, B.O. Dabbousi, M.G. Bawendi, J.J. Macklin, J.K. Trautman, T.D. Harris, L.E. Brus, Fluorescence intermittency in single cadmium selenide nanocrystals, Nature 383 (1996) 802–804.
[12] G. Schlegel, J. Bohnenberger, I. Potapova, A. Mews, Fluorescence decay time of single semiconductor nanocrystals, Phys. Rev. Lett. 88 (2002) 137401.
[13] S. Hohng, T. Ha, Near-complete suppression of quantum dot blinking in ambient conditions, J. Am. Chem. Soc. 126 (2004) 1324–1325.
[14] D.M. Warshaw, G.G. Kennedy, S.S. Work, E.B. Krementsova, S. Beck, K.M. Trybus, Differential labeling of myosin V heads with quantum dots allows direct visualization of hand-over-hand processivity, Biophys. J. 88 (2005) L30–L32.
[15] X. Gao, L. Yang, J.A. Petros, F.F. Marshall, J.W. Simons, S. Nie, In vivo molecular and cellular imaging with quantum dots, Curr. Opin. Biotechnol. 16 (2005) 63–72.
[16] J. Kurebayashi, T. Otsuki, C.K. Tang, M. Kurosumi, S. Yamamoto, K. Tanaka, M. Mochizuki, H. Nakamura, H. Sonoo, Isolation and characterization of a new human breast cancer cell line, KPL-4, expressing the Erb B family receptors and interleukin-6, Br. J. Cancer 79 (1999) 707–717.
[17] J. Kurebayashi, Regulation of interleukin-6 secretion from breast cancer cells and its clinical implications, Breast Cancer 7 (2000) 124–129.
[18] H. Kunisue, J. Kurebayashi, T. Otsuki, C.K. Tang, M. Kurosumi, S. Yamamoto, K. Tanaka, H. Doihara, N. Shimizu, H. Sonoo, Anti-HER2 antibody enhances the growth inhibitory effect of anti-oestrogen on breast cancer cells expressing both oestrogen receptors and HER2, Br. J. Cancer 82 (2000) 46–51.
[19] K. Fujimoto-Ouchi, F. Sekiguchi, Y. Tanaka, Antitumor activity of combinations of anti-HER-2 antibody trastuzumab and oral fluoropyrimidines capecitabine/5′-dFUrd in human breast cancer models, Cancer Chemother. Pharmacol. 49 (2002) 211–216.
[20] V.T. Nguyen, Y. Kamio, H. Higuchi, Single-molecule imaging of cooperative assembly of gamma-hemolysin on erythrocyte membranes, EMBO J. 22 (2003) 4968–4979.
[21] S. Toba, T.M. Watanabe, L. Yamaguchi-Okimoto, Y.Y. Toyoshima, H. Higuchi, Overlapping hand-over-hand mechanism of single molecular motility of cytoplasmic dynein, Proc. Natl. Acad. Sci. USA 103 (2006) 5741–5745.
[22] M. Ueda, Y. Sako, T. Tanaka, P. Devreotes, T. Yanagida, Single-molecule analysis of chemotactic signaling in dictyostelium cells, Science 294 (2001) 864–867.
[23] A. Yildiz, J.N. Forkey, S.A. McKinney, T. Ha, Y.E. Goldman, P.R. Selvin, Myosin V walks hand-over-hand: single fluorophore imaging with 1.5-nm localization, Science 300 (2003) 2061–2065.
[24] S. Kim, Y.T. Lim, E.G. Soltesz, A.M. De Grand, J. Lee, A. Nakayama, J.A. Parker, T. Mihaljevic, R.G. Laurence, D.M. Dor, L.H. Cohn, M.G. Bavendi, J.V. Frangioni, Near-infrared fluorescent type II quantum dots for sentinel lymph node mapping, Nat. Biotechnol. 22 (2004) 93–97.
[25] N.Y. Morgan, S. English, W. Chen, V. Chernomordik, A. Russo, P.D. Smith, A. Gandjbakhche, Real time in vivo non-invasive optical imaging using near-infrared fluorescent quantum dots, Acad. Radiol. 12 (2005) 313–323.
[26] Z. Zhelev, R. Jose, T. Nagase, H. Ohba, R. Bakalova, M. Ishikawa, Y. Baba, Enhancement of the photoluminescence of CdSe quantum dots during long-term UV-irradiation: privilege or fault in life science research? J. Photochem. Photobiol. B: Biol. 75 (2004) 99–105.
[27] K. Hanaki, A. Momo, T. Oku, A. Komoto, S. Maenosono, Y. Yamaguchi, K. Yamamoto, Semiconductor quantum dot/albumin complex is a long-life and highly photostable endosome marker, Biochem. Biophys. Res. Commun. 302 (2003) 496–501.
[28] K. Suzuki, K. Ritchi, E. Kajikawa, T. Fujiwara, A. Kusumi, Rapid hop diffusion of a G-protein coupled receptor in the plasma membrane as revealed by single-molecule techniques, Biophys. J. 88 (2005) 3659–3680.